Developmental Cell *11*, 817–829, December, 2006 ©2006 Elsevier Inc. DOI 10.1016/j.devcel.2006.09.020

A Family of Zinc-Finger Proteins Is Required for Chromosome-Specific Pairing and Synapsis during Meiosis in *C. elegans*

Carolyn M. Phillips[1] and Abby F. Dernburg[1,2,*]
[1] Department of Molecular and Cell Biology
University of California, Berkeley
Berkeley, California 94720
[2] Life Sciences Division
Lawrence Berkeley National Laboratory
Berkeley, California 94720

Summary

Homologous chromosome pairing and synapsis are prerequisite for accurate chromosome segregation during meiosis. Here, we show that a family of four related C2H2 zinc-finger proteins plays a central role in these events in *C. elegans.* These proteins are encoded within a tandem gene cluster. In addition to the X-specific HIM-8 protein, three additional paralogs collectively mediate the behavior of the five autosomes. Each chromosome relies on a specific member of the family to pair and synapse with its homolog. These "ZIM" proteins concentrate at special regions called meiotic pairing centers on the corresponding chromosomes. These sites are dispersed along the nuclear envelope during early meiotic prophase, suggesting a role analogous to the telomere-mediated meiotic bouquet in other organisms. To gain insight into the evolution of these components, we characterized homologs in *C. briggsae* and *C. remanei*, which revealed changes in copy number of this gene family within the nematode lineage.

Introduction

The cycle of sexual reproduction involves the reciprocal processes of fertilization, which unites two parental genomes, and meiosis, the specialized cell division required to partition diploid genomes to produce haploid gametes. During meiosis, a diploid germ cell undergoes a single round of DNA replication followed by two sequential divisions. At the first division, each chromosome must accurately segregate away from its homologous partner so that the resulting cells receive precisely one copy of each chromosome. Inaccuracy in this process can produce aneuploidy, which usually leads to embryonic lethality or pronounced developmental defects.

To ensure accurate homolog segregation, a series of events occurs during meiotic prophase, the endgame of which is the creation of physical links between homologous chromosome pairs. To achieve this, chromosomes must somehow contact each other and assess each other's identity, and homologous interactions must be selectively reinforced. Homolog pairing is usually stabilized by the polymerization of a proteinaceous structure between homologs (the synaptonemal complex, or SC) and later by chiasmata, the physical linkages generated through crossover recombination.

*Correspondence: afdernburg@lbl.gov

In *C. elegans*, the ability of homologs to carry out these essential steps and to segregate properly is primarily mediated by a special region near one end of each of the six chromosomes. These *cis*-acting regions are known as "homolog recognition regions" or "pairing centers" (PCs). Chromosome segments that are separated from this region by translocation or deletion can no longer recombine efficiently with homologous sequences (McKim et al., 1988; Villeneuve, 1994). These sites have at least two separable activities that promote homologous interactions: they stabilize pairing between homologs and also promote the initiation of synapsis (MacQueen et al., 2005). In addition, PCs mediate a meiotic checkpoint that monitors synapsis (Bhalla and Dernburg, 2005).

Mutations in the *C. elegans him-8* gene disrupt X-chromosome segregation, leading to a high frequency of male (XO) progeny (the "high incidence of males," or Him phenotype). We recently identified HIM-8 as a zinc-finger protein that interacts with the X chromosome PC to promote homologous synapsis during meiosis (Phillips et al., 2005). HIM-8 function is essential for all known activities of the PC on the X chromosome, including stabilization of pairing, synapsis, and activation of a checkpoint that monitors synapsis (Bhalla and Dernburg, 2005; Phillips et al., 2005). However, *him-8* mutations have no discernable effects on the segregation of the autosomes. Sex chromosomes often display unique behaviors during meiosis, particularly in the heterogametic sex. In *C. elegans*, the two X chromosomes must pair and recombine in hermaphrodites (XX) yet the single X must also segregate properly as a univalent in males (XO). It was unclear whether the role of HIM-8 is a special adaptation of the X chromosomes or an activity also required by the five autosomes.

The *him-8* gene is located in an operon with three other highly homologous predicted genes that we have named *zim* (*zinc finger in meiosis*)*-1* (T07G12.6), *zim-2* (T07G12.10), and *zim-3* (T07G12.11). Here, we demonstrate that each of the three ZIM proteins is required for meiotic pairing and synapsis of specific autosome pairs and that each protein localizes to the corresponding autosomal PCs during early prophase. Like HIM-8, the ZIM proteins are associated with the nuclear envelope during early meiosis. Comparisons among related nematode species revealed that the ZIM/HIM-8 tandem gene cluster has undergone recent changes in copy number. Taken together, these results suggest that the divergence of distinct chromosome-binding factors may enhance the fidelity of homologous interactions during meiosis, a role that could contribute to reproductive fitness and also to reproductive isolation between species.

Results

In a recent paper, we showed that HIM-8 binds to the X-chromosome PC during meiosis, is required for X-chromosome synapsis, and also mediates synapsis-independent stabilization of pairing between the X

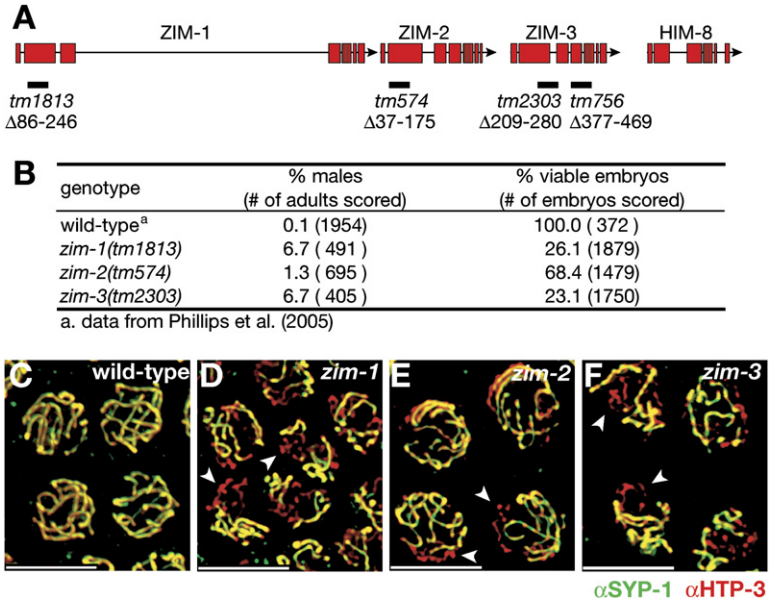

B

genotype	% males (# of adults scored)	% viable embryos (# of embryos scored)
wild-type[a]	0.1 (1954)	100.0 (372)
zim-1(tm1813)	6.7 (491)	26.1 (1879)
zim-2(tm574)	1.3 (695)	68.4 (1479)
zim-3(tm2303)	6.7 (405)	23.1 (1750)

a. data from Phillips et al. (2005)

Figure 1. Deletion of *zim-1*, *zim-2*, or *zim-3* Results in Meiotic Chromosome Missegregation and Unsynapsed Chromosomes

(A) Diagram of the ZIM/HIM-8 operon indicating the region of each gene removed by the deletion alleles described here. *zim-3(tm756)* is an in-frame deletion, while *zim-1(1813)*, *zim-2(tm574)*, and *zim-3(tm2303)* result in frame shifts and early stop codons. Zn finger regions are indicated by darker red shading.

(B) Frequencies of males and viable embryos observed among whole broods in wild-type, *zim-1*, *zim-2*, and *zim-3* hermaphrodites.

(C–F) Pachytene nuclei showing immunofluorescence of SYP-1 (green) and HTP-3 (red) for each indicated genotype. (C) Wild-type nuclei display extensive colocalization of SYP-1 and HTP-3 along the lengths of all six chromosomes. (D–F) In *zim-1*, *-2*, and *-3* mutants, unsynapsed chromosomes are detected at pachytene as segments that stain with HTP-3 (red) but not SYP-1 (green). Arrowheads indicate particularly clear examples of unsynapsed chromosomes. All images are projections of deconvolved 3D images. Scale bars represent 5 μm.

chromosomes (Phillips et al., 2005). It was curious that loss of HIM-8 only impairs segregation of the X chromosomes yet is required for meiotic functions that are shared by all chromosomes; that is, all chromosomes must pair and synapse with their homologs to segregate properly in *C. elegans.* This raised the question of whether there might exist autosomal counterparts to HIM-8 that mediate pairing and synapsis.

Genome annotations based on gene predictions and cDNA evidence suggested that *him-8* is one of four related genes within a tandem array (Figure 1A). Analysis of transcripts from these genes indicated that they are likely coexpressed as an operon (Blumenthal et al., 2002). The four genes share similar C-terminal regions encoding two noncanonical C2H2 zinc fingers. They also share strong similarity in their N-terminal portions, which lack obvious structural motifs but contain numerous potential modification sites. Based on their similarity to each other and the analysis described here, we have named these genes *zim-1*, *-2*, and *-3* (for "*zinc finger in meiosis*"); the numbering reflects their order in the genome.

Due to extensive homology in their coding sequences, we could not obtain unequivocal functional information about the individual genes by RNAi-mediated knockdown. However, individual deletion alleles of each of the three genes were successfully isolated by the Japanese National Bioresource for *C. elegans* (Figure 1A). To gain further insight into the mechanism of homolog pairing and synapsis, we have studied the effects of these mutations on meiotic chromosome behavior. We also raised antibodies specific for each of the three ZIM proteins to investigate their localization during meiosis.

Mutations in the *zim* Genes Result in Meiotic Defects

Deletions in each of the three *zim* genes were isolated by PCR screening of mutagenized worm libraries (Gengyo-Ando and Mitani, 2000). Once the individual mutations were outcrossed to eliminate background effects (see Experimental Procedures), we found that hermaphrodites homozygous for *zim-1(tm1813)*, *zim-2(tm574)*, and *zim-3(tm2303)* were morphologically normal and fertile but gave rise to broods containing both inviable progeny (embryos that fail to hatch) and an elevated incidence of males. Taken on its own, embryonic inviability is a fairly uninformative phenotype since it can result from anueploidy due to chromosome missegregation during meiosis but can also reflect loss of factors required for early development. However, the high incidence of male progeny, or "Him," phenotype is diagnostic for meiotic X-chromosome segregation defects. We quantified the frequency of males and inviable progeny (Figure 1B) and found that *zim-1* and *zim-3* were quantitatively very similar, but *zim-2* mutants produced substantially fewer males and more viable progeny than either of the other mutants. Mutations in *him-8*, which abrogate X-chromosome pairing and synapsis, result in ~40% male progeny and nearly 100% viable embryos (Phillips et al., 2005). Therefore, segregation of the X chromosome does not depend nearly as strongly on *zim-1*, *-2*, or *-3* as it does on *him-8*. On the other hand, the inviability among the progeny of *zim* mutants indicated that these genes might be important for autosomal segregation.

To determine whether lethality among the progeny of *zim* mutants arises from segregation defects during meiosis, we directly examined chromosome behavior during meiotic prophase. To evaluate synapsis, we performed immunofluorescence detection of two components of the SC. HTP-3 is an axial component that localizes to meiotic chromosomes prior to synapsis, while SYP-1 is a central element protein that loads during synapsis (MacQueen et al., 2002, 2005). By definition, chromosomes or chromosome segments that load HTP-3 but not SYP-1 are unsynapsed. By this assay, *zim-1*, *zim-2*, and *zim-3* mutants consistently exhibited unsynapsed chromosomes in their pachytene-stage nuclei (Figures 1C–1F), implicating each of the *zim* genes in homolog pairing and/or synapsis.

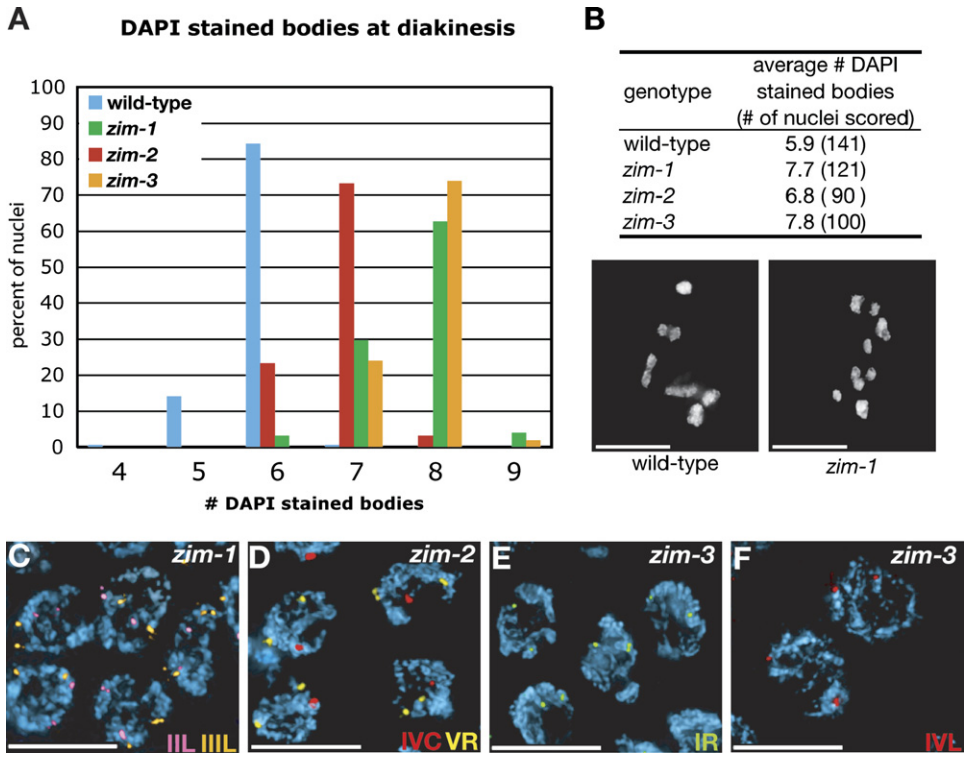

Figure 2. *zim* Mutants Display Chromosome-Specific Defects in Synapsis and Chiasma Formation

(A) Wild-type oocytes stained with DAPI display six bivalents at diakinesis, representing the six pairs of homologous chromosomes held together by chiasmata. The number of DAPI-stained bodies can be underestimated when bivalents lie too close to be visually resolved. The histogram indicates the distribution of oocyte nuclei with various numbers of DAPI-stained bodies for wild-type hermaphrodites and the three *zim* mutants.
(B) Mean number of DAPI-stained bodies detected for the genotypes shown in (A). A typical wild-type oocyte with six DAPI-stained bodies and a *zim-1* mutant oocyte with eight DAPI-stained bodies are shown below.
(C–F) Pachytene-stage nuclei from samples hybridized with fluorescent DNA probes specific for different chromosomes. These and other experiments indicated that particular chromosomes consistently fail to synapse in each of the zim mutants. (C) In *zim-1* mutants, probes to the left ends of chromosomes II (pink) and III (orange) are unpaired in the pachytene region. (D) In *zim-2* mutants, a probe to the right end of chromosome V (yellow) is unpaired, while a probe to the center of chromosome IV (red) is paired in the pachytene region. (In this example, the IVC probe is a positive control.) (E and F) Probes to chromosomes I (E, green) and IV (F, red) are unpaired at pachytene in *zim-3* mutants. Scale bars represent 5 μm.

Visual examination of oocytes at the diakinesis stage of meiosis, which occurs near the end of prophase shortly before the first meiotic division, can also reveal defects in pairing and synapsis. By this stage, the SC has largely disassembled, and pairwise interactions between homologous chromosome pairs are maintained by chiasmata. Accordingly, six bivalents, corresponding to the five autosome pairs and single pair of sex chromosomes, are normally observed. Nonrecombinant, or achiasmate, chromosomes are detected as extra DAPI-stained bodies (univalents). This assay is less specific than direct visualization of homolog synapsis since univalents can also result from defects in recombination or cohesion, but the number of DAPI-stained bodies can be quantified more precisely than unsynapsed chromosomes. Most nuclei in *zim-2* mutants contained seven DAPI-stained bodies, representing five bivalents and two univalents, whereas *zim-1* and *zim-3* mutants most frequently had eight DAPI-stained bodies (Figures 2A and 2B).

The frequency of either bivalents or viable progeny in each of the *zim* mutants is inconsistent with a complete failure in chromosome synapsis. The mixture of bivalents and achiasmate chromosomes in *zim* mutants could indicate that the proteins act combinatorially to promote synapsis and that loss of any one of their functions reduces the probability of synapsis of each chromosome pair. However, if the *zim* mutations had a probabilistic effect on pairing and synapsis of each autosome, we would expect a Poisson distribution of univalent chromosomes, which is not what was observed. The tight frequency distribution of achiasmate chromosomes in each of the *zim* mutants is more consistent with the idea that each of the mutations potently impairs synapsis of a limited number of chromosomes.

Each *zim* Gene Is Responsible for Synapsis of Specific Autosome Pairs

To identify the chromosomes affected by each of the *zim* mutations, we performed FISH with probes specific for each of the six chromosomes to assess homologous interactions at the pachytene stage, where all chromosomes are normally paired and synapsed. In *zim-2* hermaphrodites, a probe to chromosome V consistently displayed two unpaired FISH signals at pachytene, while probes to all other chromosomes were paired. By

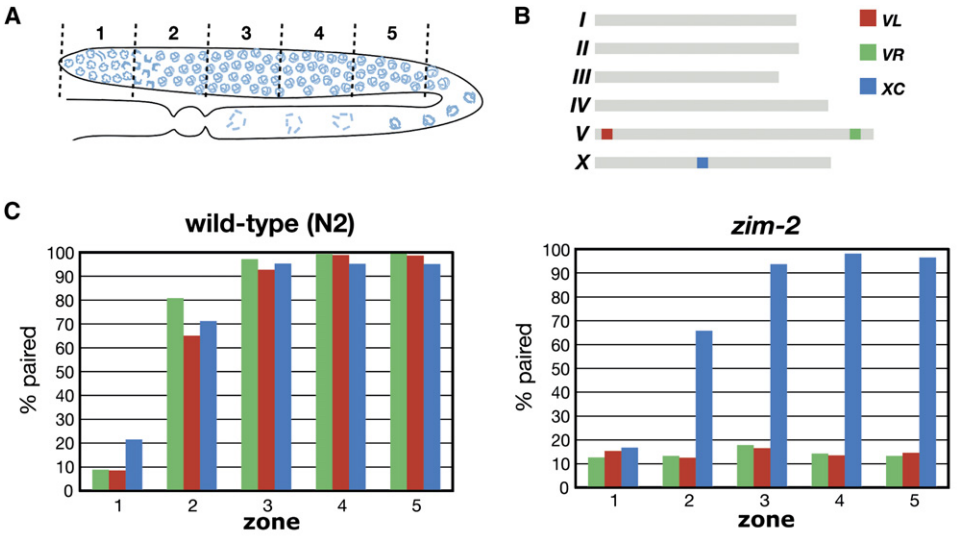

D

VR	1	2	3	4	5
wild-type (N2)	8.9 (349)	80.9 (424)	97.2 (498)	99.3 (443)	100 (305)
zim-2 (tm574)	12.7 (292)	13.3 (278)	17.9 (302)	14.3 (280)	13.4 (232)

VL	1	2	3	4	5
wild-type (N2)	8.6 (349)	64.9 (424)	92.8 (498)	98.9 (443)	98.7 (305)
zim-2 (tm574)	15.4 (292)	12.6 (278)	16.6 (302)	13.6 (280)	14.7 (232)

XC	1	2	3	4	5
wild-type (N2)	21.5 (349)	71.2 (424)	95.4 (498)	95.3 (443)	95.1 (305)
zim-2 (tm574)	16.8 (292)	65.8 (278)	93.7 (302)	98.2 (280)	96.6 (232)

Figure 3. Pairing of Chromosome V Is Not Stabilized in *zim-2* Mutants

(A) Diagram of a hermaphrodite gonad, indicating the five zones in which homolog association was scored.

(B) Genomic locations of the three FISH probes used to quantify homolog pairing.

(C) The bar graphs indicate the fraction of paired FISH signals in each zone for wild-type (N2) and *zim-2(tm574)* hermaphrodites. Three probes were scored independently in the same samples: they marked the left end of chromosome V (red), the right end of chromosome V (green), and the center of the X chromosome (blue). In *zim-2*, pairing of the chromosome V probes did not rise above the baseline levels observed in the premeiotic region (zone 1), whereas the X-chromosome-association rates and dynamics were very similar to what we observed in wild-type hermaphrodites.

(D) Data corresponding to the graphs in (C) indicate the frequency of paired signals (and number of nuclei examined).

contrast, in *zim-1* and *zim-3* mutants, probes to two different chromosome pairs, II and III for *zim-1* and I and IV for *zim-3*, were abnormally separated at pachytene (Figures 2C–2F). In all *zim* mutants, the X chromosomes synapsed normally. While there may be subtle effects on the X chromosome that are not easily detected cytologically, we favor the idea that the elevated frequencies of X missegregation observed in the *zim* mutants are an effect of autosomal asynapsis (see Discussion).

This analysis implicates each of the *zim* genes in the synapsis of either one or two autosome pairs. Conversely, it reveals that each of the five autosomes is acutely affected by one and only one of the *zim* genes. *zim-2* affects only one chromosome pair, while *zim-1* and *zim-3* mutations each perturb two autosomes. This agrees well with the numbers of bivalents and univalents seen at diakinesis in each of the mutants and can also explain the greater embryonic lethality observed for *zim-1* and *zim-3* compared to *zim-2*.

Pairing of Chromosome V Is Disrupted in the *zim-2* Mutant

To ascertain whether *zim* mutants are defective in homolog pairing or specifically fail to initiate synapsis, we analyzed the dynamics of homolog pairing in *zim-2* mutants through temporal analysis. Homologous interactions were quantified as a function of prophase progression in fixed, whole-mount gonads by analyzing the frequency of paired FISH probes in five sequential intervals (Figure 3A). The most distal zone includes premeiotic nuclei, which are undergoing mitotic proliferation. Zone 2 includes mostly nuclei at the leptotene/zygotene stage, during which homologs pair and initiate synapsis. Zones 3–5 represent the pachytene region, where chromosomes are normally fully aligned and synapsed with their homologs.

Fluorescent probes to the left and right ends of chromosome V were hybridized to dissected wild-type and *zim-2* gonads. A probe that hybridizes to the center of

the X chromosome was included for comparison (Figure 3B). The fraction of nuclei containing paired FISH signals was measured for each zone. In wild-type control animals, all three FISH probes showed only infrequent homolog associations in zone 1, but in zone 2, paired FISH signals began to appear, as previously described (MacQueen et al., 2002; Phillips et al., 2005). By zone 3, pairing and synapsis are normally complete, as detected by nearly 100% paired probes. In *zim-2* hermaphrodites, interactions between X chromosomes progressed normally, but pairing of chromosome V was severely compromised, as reflected by the observation that neither probe ever showed a frequency of pairing above the background level seen in the premeiotic region (Figures 3C and 3D).

In mutants such as *syp-1* and *syp-2* that abrogate synapsis, pairing at the PC ends of chromosomes is stabilized relative to pairing at non-PC ends (Colaiacovo et al., 2003; MacQueen et al., 2002) This "synapsis-independent stabilization of pairing" requires an interaction between homologous PCs (MacQueen et al., 2002, 2005). Stabilization of pairing at the PC end of the X chromosome also requires HIM-8 (Phillips et al., 2005). Our findings indicate that ZIM-2, like HIM-8, is required both for synapsis-independent stabilization of pairing and for synapsis of a specific chromosome pair and therefore that the stabilization of X chromosome pairing does not involve a unique mechanism.

ZIM Proteins Bind to the Pairing Centers of the Autosomes They Control

To investigate the localization of the ZIM proteins, polyclonal antisera were raised against synthetic peptides corresponding to regions of minimal conservation at the C termini of each protein (see Experimental Procedures). Each of the three antisera localized to discrete chromosome-associated foci that were most prominent in the transition zone and very early pachytene (Figure 4A). To validate the specificity of the antisera, we performed immunolocalization in mutant animals. *him-8(mn253)*, *zim-1(tm1813)*, *zim-2(tm574)*, and *zim-3(tm2303)* mutants were dissected and stained with each the ZIM antibodies as well as the HIM-8 antibody (Phillips et al., 2005). In each case, the mutation abrogated staining of the corresponding protein, but each of the other three proteins could be detected as subnuclear foci, indicating that each of the four proteins localizes to meiotic chromosomes independently of the other three family members (Figure 6B).

At the onset of meiosis, ZIM-2 was detected at no more than two foci. By early pachytene, ZIM-2 was consistently detected as a single focus in each nucleus (Figure 4C). By contrast, ZIM-1 and ZIM-3 often localized to three to four foci at the onset of meiosis and, by early pachytene, were usually observed at two foci (Figures 4B and 4D). Based on the knowledge that HIM-8 associates with the X-chromosome PC, we considered it highly likely that the foci of ZIM-1, -2, and -3 proteins corresponded to autosomal PCs, most probably to the chromosomes that missegregate in the corresponding mutants. This hypothesis was validated by combining immunofluorescence detection of each ZIM protein with FISH to the PC of each autosome. These colocalization experiments revealed clear correspondence of ZIM-1 with the left ends of both chromosome II and chromosome III (Figures 5A–5D), ZIM-2 with the right end of chromosome V (Figures 5E–5H), and ZIM-3 with the right end of chromosome I and the left end of chromosome IV (Figures 5I–5P). Taken together, these observations indicate that the ZIM proteins are functional paralogs of HIM-8 that bind to the PCs of specific chromosomes and are required on those chromosomes to mediate meiotic chromosome pairing and synapsis (Figure 5Q).

Pairing Centers Associate with the Nuclear Envelope but Do Not Cluster

Like HIM-8, all ZIM protein foci were consistently observed at the nuclear periphery in early prophase nuclei, suggesting a physical association with the nuclear envelope. This was even more evident in samples stained with antibodies to ZIM proteins and nuclear lamin (Figures 4E–4G). All PCs are therefore associated with the nuclear envelope during the stages of homolog pairing and synapsis initiation.

One notable difference among the four members of this family is that bright, nuclear-envelope-associated HIM-8 foci are clearly detected through the end of pachytene (Phillips et al., 2005). By contrast, ZIM protein foci become much less prominent by midpachytene, after the completion of chromosome synapsis. However, more diffuse chromatin-associated staining was detected through the end of pachytene, suggesting that the ZIM proteins may lose their ability to concentrate at specific nuclear envelope sites but retain chromosome binding activity after synapsis is complete (Figure S1A available with this paper online).

Interestingly, we observed that in *chk-2(me64)* mutants, which lack a transition zone and fail to pair or synapse their chromosomes (MacQueen and Villeneuve, 2001), the subnuclear localization of the three ZIM proteins throughout the gonad resembled their normal post-synapsis localization in wild-type animals, in that the proteins did not appear as bright nuclear-envelope-associated foci, although they could be detected on chromosomes (Figure S1B). We interpret this to mean that ZIM-1, -2, and -3 concentrate at nuclear-envelope sites in a CHK-2-dependent manner. By contrast, HIM-8 concentration at the nuclear envelope is retained in *chk-2* mutants (Phillips et al., 2005). This provides further evidence that the ZIMs and HIM-8 may be controlled by distinct, likely posttranslational, regulatory mechanisms.

During meiotic prophase in diverse organisms, telomeres associate with the nuclear envelope and cluster together transiently in a configuration known as the meiotic bouquet (reviewed by Scherthan [2001]). We therefore tested whether the twelve chromosomal PCs, as detected by the four ZIM/HIM-8 antibodies, are clustered during early prophase. Gonads were stained with all compatible combinations of antibodies (Figure 6B shows some examples in *zim* mutants; data for wild-type animals not shown). The staining of each ZIM protein was not correlated with other ZIMs or with HIM-8. When wild-type hermaphrodites were costained with all three ZIM antibodies and the HIM-8 antibody, multiple dispersed foci were detected at the periphery of each nucleus during early prophase (Figure 6C), further indicating that these sites do not concentrate at one region of the nuclear envelope.

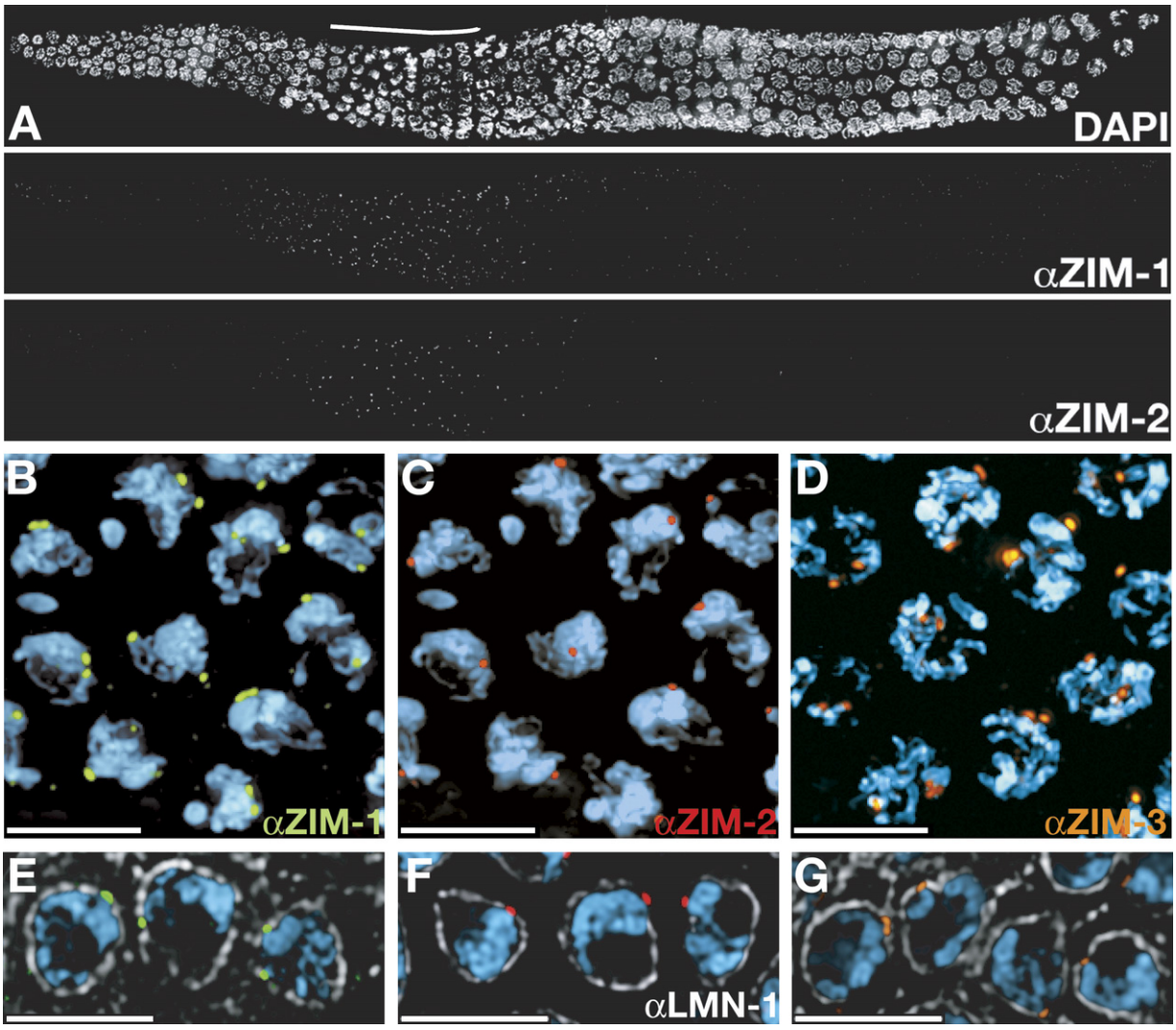

Figure 4. ZIM Proteins Localize to Discrete Foci at the Nuclear Envelope during Early Meiotic Prophase

(A) Wild-type gonad stained with DAPI and antibodies to ZIM-1 and ZIM-2. Foci are most apparent in the transition zone of the gonad (indicated by white bar). Some signals can be seen outside the transition zone/early pachytene region, but most of these do not correspond to DAPI-stained regions and thus are likely nonspecific background.

(B and C) In the latter portion of the transition zone, most nuclei have two foci of ZIM-1 (B, green) and a single focus of ZIM-2 (C, red).

(D) In early pachytene, two foci of ZIM-3 (orange) can been visualized in each nucleus.

(E–G) Optical sections showing wild-type pachytene nuclei stained with antibodies against nuclear lamin/LMN-1 (white), ZIM-1 (E, green), ZIM-2 (F, red), and ZIM-3 (G, orange). These cross-sections reveal the close juxtaposition of the ZIM proteins with the lamina more clearly than projections through the entire nuclear volume, but not all ZIM-1 and ZIM-3 foci are visible within the shallow focal plane. Scale bars represent 5 μm.

We considered the possibility that clustering of PCs might occur only transiently during homolog pairing. If so, it seemed likely that mutations that inhibit synapsis and consequently extend the leptotene/zygotene stage might prolong a normally transient clustering phase. Therefore, we examined at HIM-8 and ZIM protein foci in *syp-1(me17)* and *syp-2(ok307)* loss-of-function mutants, which abrogate synapsis and result in an extended region of polarized nuclei (Colaiacovo et al., 2002; MacQueen et al., 2002). We also tested *rec-8(ok978)* mutants since in budding yeast, *Rec8* mutations result in a prolonged bouquet cluster (Trelles-Sticken et al., 2005). Clustering of the ZIM and HIM-8 signals was not observed in any of these mutants (data not shown). Interestingly, in *syp-1* and *syp-2* hermaphrodites, distinct, nuclear-envelope-associated foci for each ZIM protein persisted throughout the extended region of polarized nuclei. At this time, we do not know whether the association of ZIM proteins with the nuclear envelope is a cause or a consequence of the polarized configuration of chromosomes observed in *C. elegans* meiotic nuclei prior to completion of synapsis.

We also noted that each of the *zim* mutations themselves resulted in an extended region of polarized nuclei, as previously observed for *him-8* mutants (compare Figure 6A to Figure 4A) (Phillips et al., 2005). This observation indicates that persistent polarization can be triggered by asynapsis of any pair of chromosomes. Prominent foci of other ZIM proteins persisted throughout this extended polarized region (Figure 6A), implying that the dispersal of ZIM proteins from nuclear envelope foci is coupled to the global loss of nuclear polarization

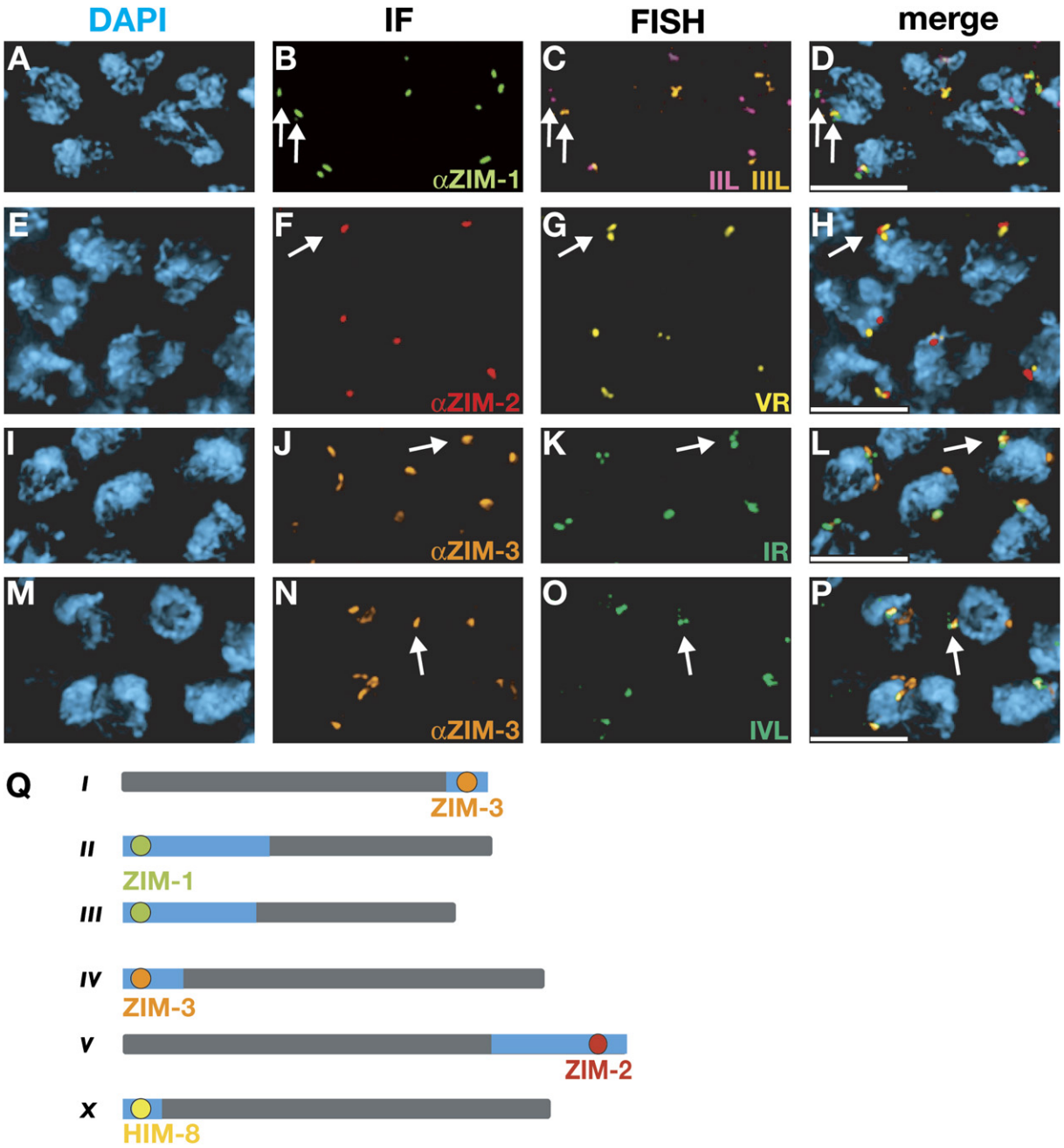

Figure 5. ZIM Proteins Localize to Autosomal Pairing Centers

(A–D) ZIM-1 colocalizes the left ends of chromosomes II and III. Two arrows point to the two ZIM-1 foci in a single nucleus and to the chromosomes II and III FISH probes, which colocalize with them.

(E–H) ZIM-2 colocalizes with a FISH probe to the right end of chromosome V. A particularly clear example of this colocalization is indicated by the arrow.

(I–P) ZIM-3 colocalizes with FISH probes to the right end of chromosome I (I–L) and the left end of chromosome IV (M–P). Arrows point to clear examples. (A, E, I, and M) Late transition zone or early pachytene nuclei stained with DAPI. (B, F, J, and N) Immunolocalization of ZIM-1, ZIM-2, ZIM-3, and ZIM-3, respectively. (C, G, K, and O) FISH signals corresponding to IIL, IIIL, VR, IR, and IVL. (D, H, L, and P) Merged images.

(Q) Correspondence of ZIM-1, -2, -3, and HIM-8 to the PC regions of the six *C. elegans* chromosomes. The region to which the PCs have been mapped genetically are demarcated in blue. Scale bars represent 5 μm.

upon completion of synapsis rather than synapsis of the individual chromosomes to which they are bound.

Evolution of the ZIM/HIM-8 Protein Family

Because *zim-1*, *zim-2*, *zim-3*, and *him-8* share extensive structural and functional similarities and are organized as a tandem gene array, they have likely arisen from a common ancestor through gene duplication, divergence, and selection. To learn more about the evolution of this family of proteins, we identified and characterized homologous genes in two related nematode species, *C. remanei* and *C. briggsae*, for which extensive

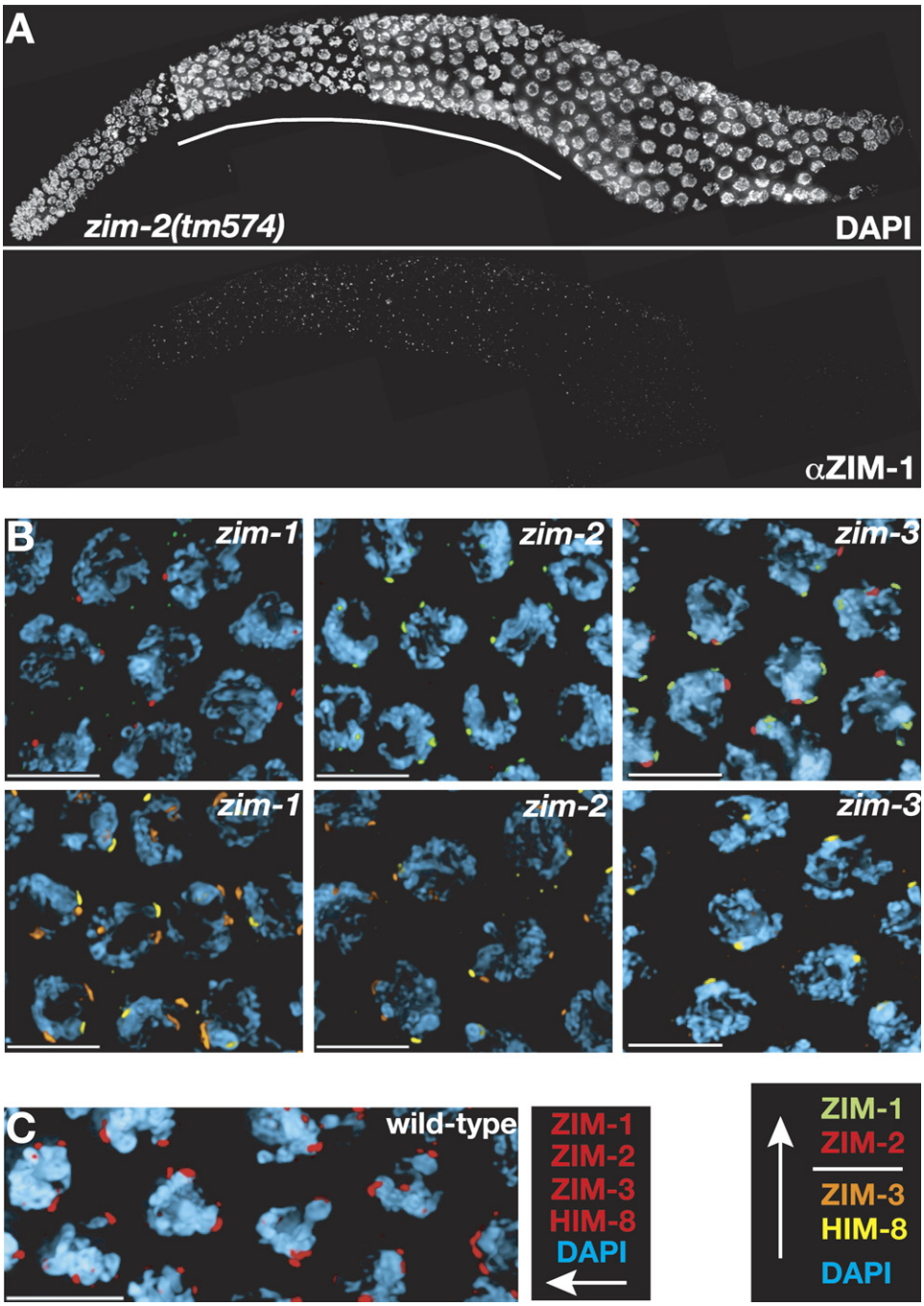

Figure 6. ZIM-1, ZIM-2, and ZIM-3 Recognize Distinct Chromosomal Foci and Do Not Cluster in Meiotic Nuclei

(A) Gonad from a *zim-2* hermaphrodite stained with DAPI and ZIM-1 shows an extended region of polarized nuclei (indicated by white line) and increased perdurance of ZIM-1 foci relative to wild-type (compare to Figure 4A).

(B) Immunofluorescence of ZIM-1 (green) and ZIM-2 (red) (top three panels) and ZIM-3 (orange) and HIM-8 (yellow) (bottom three panels) in *zim-1*, *zim-2*, and *zim-3* meiotic nuclei. In each case, the mutation eliminates detection of the corresponding protein, but the other three proteins show normal subnuclear staining.

(C) Wild-type transition zone nuclei stained antibodies against ZIM-1, ZIM-2, ZIM-3, and HIM-8 show multiple foci dispersed along the nuclear periphery, indicating a lack of tight clustering among the different PCs. Scale bars represent 5 μm.

genome sequence is available. In each case, homology searches identified one or more contigs that encode apparent orthologs of the *C. elegans* genes, but some gap filling was required to complete and annotate the sequence of the syntenic regions (see Experimental Procedures).

This analysis revealed the presence of four *zim/him-8* genes in *C. remanei* and five in *C. briggsae* (GenBank accession numbers DQ498827 and BK005903, and Supplemental Data). In both species, as in *C. elegans*, all genes are closely spaced in a tandem array, suggesting that their operon organization is conserved

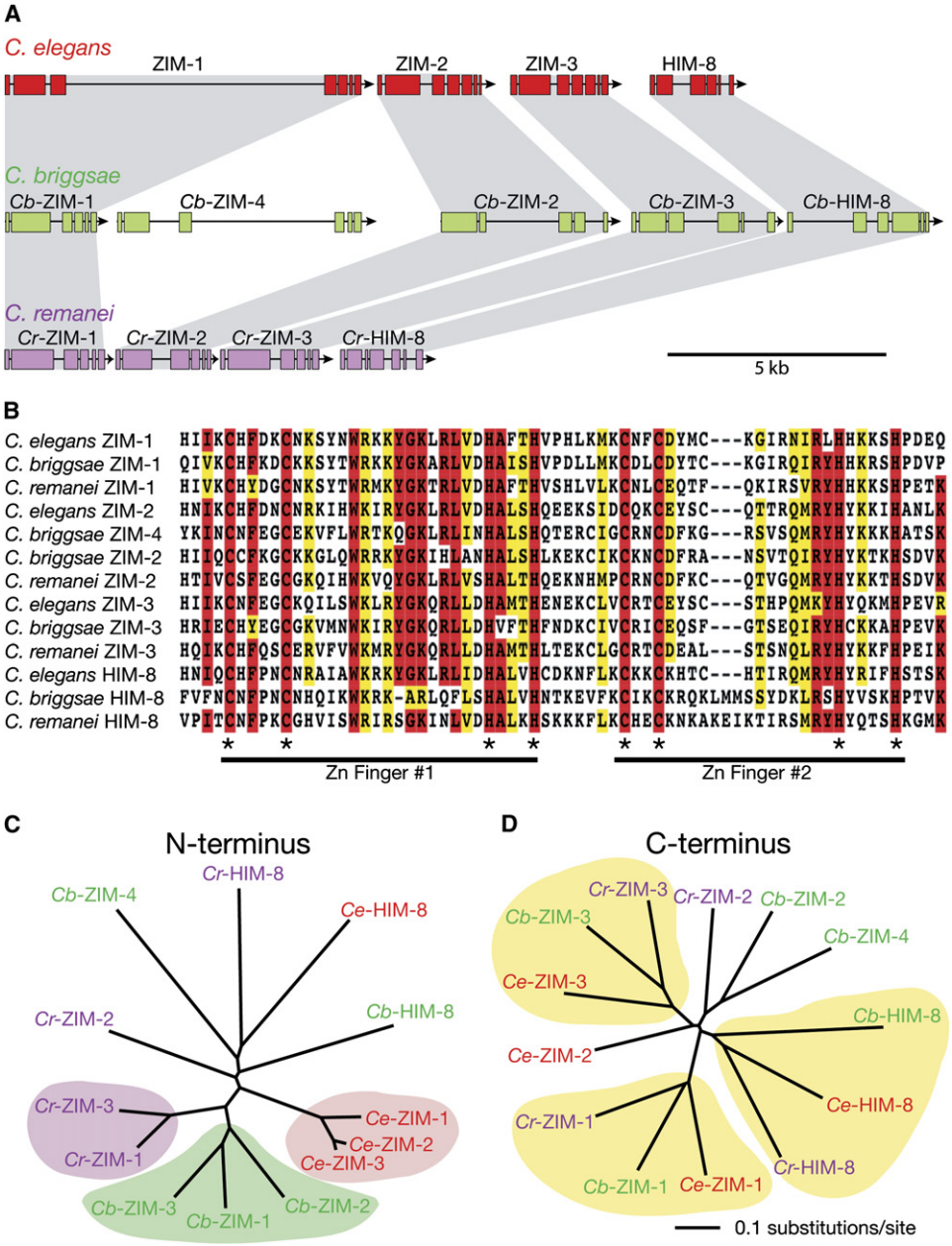

Figure 7. Evolution of the ZIM/HIM-8 Protein Family

(A) Schematic of the ZIM/HIM-8 gene cluster in *C. elegans*, *C. briggsae*, and *C. remanei.* Predicted orthologs based on sequence comparisons are linked by gray shading.

(B) ClustalX alignment of the Zn finger region of all ZIM/HIM-8 proteins from *C. elegans*, *C. briggsae*, and *C. remanei.* Red and yellow shading indicate identical and similar residues, respectively. Asterisks mark zinc coordinating residues.

(C and D) Unrooted trees of the ZIM/HIM-8 proteins generated with ClustalX and TREEVIEW. (C) Phylogenetic relationships among the ZIM/HIM-8 proteins based on analysis of the N-terminal (non-zinc finger) region. Color-coded regions highlight branches of the tree that reveal greater conservation of this domain within individual species than between species. (D) Phylogenetic tree derived from the conserved C-terminal region of the ZIM/HIM-8 proteins, including two C2H2 Zn fingers. Yellow shading highlights branches of the tree that reveal orthologous relationships among ZIM proteins from different nematode species.

(Blumenthal et al., 2002) (Figure 7A). The difference in gene number does not reflect a difference in the karyotypes of these species since visualization of bivalents at diakinesis revealed that all three have six chromosome pairs (Figures S2A, S2B, and S2D).

To analyze the ZIM/HIM-8 proteins in the three nematodes, multiple alignments were calculated with ClustalX and used to generate phylogenetic trees (Chenna et al., 2003; Thompson et al., 1994). Using these tools, we identified orthologous relationships among the genes in the three species. The portion of the alignment containing the zinc fingers is shown in Figure 7B.

Amino acid sequence alignments revealed blocks of strong conservation in the N- and C-terminal portions of the proteins. Using the neighbor-joining method, we generated separate trees for each of these conserved

domains (Figure 7C). The C-terminal region containing the two zinc fingers showed greatest conservation among the corresponding proteins in the other two species, but the N termini were more closely related to the other ZIM/HIM-8 proteins within the same species. We hypothesize that the zinc fingers have retained their individuality as distinct sequence-binding motifs, while the N termini within each species are likely coevolving with a common set of interacting proteins. Based on comparisons of this C-terminal region, the order of genes within the tandem array is conserved in each species, with *him-8* as the most downstream gene. However, *C. briggsae* has an additional gene located between the orthologs of *zim-1* and *zim-2* (Figure 7A).

Computational identification of *him-8* in *C. briggsae* was ambiguous, both because of greater sequence divergence from *C. elegans* and also because of the extra gene relative to the other two species. To validate our assignments of the *C. briggsae* genes, we carried out RNAi to inactivate both the last gene in the operon and the gene we identified as unique to *C. briggsae*, based on its divergence from the *C. elegans* and *C. remanei* genes. Double-stranded RNA corresponding to regions of these genes sharing minimal nucleotide sequence similarity with other family members was injected into adult *C. briggsae* hermaphrodites (see Experimental Procedures). Progeny of the injected animals were analyzed for meiotic chromosome segregation defects, particularly an increase in the incidence of males among their offspring (i.e., males in the F2 generation). In addition, we examined the number of DAPI-stained bodies at diakinesis among the F1 generation.

Inactivation of the downstream gene in *C. briggsae* by RNAi resulted in F1 animals with a strong Him phenotype. We saw a high variance in the frequency of male production, presumably due to the variability inherent in RNAi experiments, but the most severely affected animals produced 22%–31% males (Figures S2D and S2E). Cytological analysis revealed that these F1 animals usually had seven DAPI-stained bodies at diakinesis, indicating a single pair of nonrecombinant chromosomes (Figures S2D and S2F). Together, these data indicate that this gene specifically affects X-chromosome synapsis, corroborating the identification of this gene as *Cb-him-8*.

We did not observe meiotic defects following RNAi of the gene we have named *Cb-zim-4*. Oocyte nuclei from these hermaphrodites usually had six DAPI-stained bodies at diakinesis (Figures S2D and S2F), as did uninjected controls, indicating that all chromosome pairs efficiently underwent pairing, synapsis, and crossing over. These results may indicate that the gene lacks an essential role in meiotic pairing and synapsis, perhaps because it has diverged recently and shares functional redundancy with another *C. briggsae* gene. Alternatively, we may not have effectively knocked down the function of this gene by RNAi.

Discussion

Chromosome Specificity of the ZIM Proteins and Their Role in Partner Recognition

Together with a previous study (Phillips et al., 2005), the experiments described here show that each chromosome in *C. elegans* requires the activity of a specific member of the ZIM/HIM-8 protein family to mediate efficient meiotic pairing and synapsis. These proteins localize to the genetically defined PC regions of the corresponding chromosomes, perhaps by binding to specific sequences enriched within these regions. Like HIM-8, ZIM-2 localizes to a single pair, chromosome V, while ZIM-1 and ZIM-3 each localize to two chromosome pairs.

Our cytological experiments reveal no obvious overlap in the localization of the distinct ZIM/HIM-8 proteins. Together with evidence that each protein localizes to chromosome sites independently of the others, this argues against the idea that the proteins behave in a combinatorial fashion on any of the six chromosomes. Furthermore, the effects of HIM-8 and the three ZIM proteins on pairing and synapsis are specifically restricted to those chromosomes where we detect their localization. Nevertheless, hermaphrodites that lack *zim-1*, *zim-2*, or *zim-3* activity produce male self-progeny at a level significantly above that of wild-type animals, although well below the frequency of *him-8* mutants (Figure 1B). Since unpaired X-chromosome FISH signals were not detected at elevated frequencies in any of the *zim* mutants, we favor the idea that these segregation errors may be indirect consequences of loss of ZIM function.

In wild-type animals, there is likely to be a low but nonzero incidence of oocytes with aberrant X-chromosome synapsis or recombination. Normally, these anomalies are evidently removed by meiotic checkpoints that trigger apoptosis since apoptosis-deficient hermaphrodites (e.g., *ced-4* mutants) produce 1% male progeny, an order of magnitude above wild-type animals (Bhalla and Dernburg, 2005). *zim-2* mutants produce a similar level of males (1.3%), which may arise in an analogous way, if the presence of unsynapsed autosomes (Vs) in every nucleus "masks" the rare X aberrations from detection by meiotic checkpoints. In an experiment described in the online Supplemental Data, we provide direct evidence that meiotic checkpoints can strongly influence the distribution of progeny among *zim-2* mutants (Figure S3).

The X nondisjunction seen in *zim-1* and *zim-3* mutants (which have two pairs of unsynapsed autosomes) is markedly higher (6.7% males) and cannot be entirely accounted for by loss of checkpoint filtering. We speculate that the presence of multiple univalents during the MI division may perturb chromosome congression or the ability of the meiotic spindle to accurately segregate either achiasmate X chromosomes or X bivalents with a suboptimal chiasma position. Precedence for this idea comes from analysis of meiotic chromosome segregation in both *Drosophila* females and budding yeast, where a single pair of achiasmate chromosomes will segregate very regularly, but multiple pairs of achiasmate chromosomes quickly "saturate" the backup segregation systems and lead to greatly elevated nondisjunction (Baker et al., 1976; Ross et al., 1996). This idea is supported by the higher frequency of male production in *zim-1* and *zim-3*, which have two pairs of achiasmate chromosomes, compared to *zim-2*, with only a single pair of achiasmate chromosomes. The greater-than-double number of inviable embryos in *zim-1* and *zim-3* compared to *zim-2* (Figure 1B) might also reflect more

chaotic chromosome congression or segregation due to two pairs of achiasmate chromosomes.

It is not obvious why some chromosomes have unique PC binding proteins, yet two pairs of autosomes each share a single protein. We have tested whether nonhomologous chromosomes that share a ZIM protein, i.e., chromosomes II and III or I and IV, undergo appreciable levels of nonhomologous synapsis, but we have never observed such a configuration in wild-type animals (data not shown). Along with prior evidence, this indicates that the specificity of homolog recognition cannot be solely defined by either by the role of the PCs or the identity of the corresponding ZIM/HIM-8 family member. The basis for homolog recognition during meiotic pairing remains unknown. Indeed it is not yet clear whether this process is mediated purely by protein-based mechanisms or if it requires base-pairing interactions between potential partner chromosomes. It also remains ambiguous whether all organisms share the same mechanism of partner recognition, especially since homolog pairing requires double-strand breaks in many organisms, including budding yeast, *Arabidopsis*, and mice, but not in an others, such as the metazoans *C. elegans* and *Drosophila* (reviewed by Gerton and Hawley [2005]). Although meiotic double-strand breaks are not required for pairing and synapsis in *C. elegans* (Dernburg et al., 1998), it remains possible that the recombination machinery plays a role in partner discrimination.

Conservation of ZIM Protein Function within and Beyond the Nematode Lineage

Analysis of ZIM/HIM-8 homologs in related species reveals that (1) different domains of the proteins show distinct patterns of conservation and divergence within and between the species, and (2) the number of genes in the family is not static and is likely increasing. The second conclusion is based on knowledge that *C. briggsae* and *C. remanei* are more closely related to each other than either species is to *C. elegans* (Kiontke et al., 2004). It is therefore more parsimonious to propose that the extra *zim* gene in *C. briggsae* has resulted from a recent gene duplication than independent instances of gene loss in *C. remanei* and *C. elegans.*

It seems most likely that the ZIM/HIM-8 family in *C. elegans* represents an intermediate state in evolution. We imagine that there was originally a single member of the ZIM/HIM-8 family that bound to all chromosomes, but the duplication and divergence of the protein family (in concert with their binding sites) gradually enhanced either the speed or accuracy of the process of meiotic pairing and synapsis. We predict that a distinct PC binding protein for each of the six chromosomes would be a more optimal situation and that *C. briggsae*, with five family members, may be one step closer to this condition than *C. elegans* or *C. remanei*.

Cb-zim-4 is most closely related to the adjacent *Cb-zim-2* gene, based primarily on similarity in their zinc fingers. In other examples of zinc-finger gene clusters, new genes tend to be adjacent to their parent and likely arise through single gene-duplication events (Shannon et al., 2003). Our RNAi experiments did not reveal whether *Cb-zim-4* encodes a functional gene product. It is possible that this gene represents an intermediate in the process of acquiring a unique function and is either redundant with *Cb-zim-2* or nonfunctional. It has been noted that clusters of Zn finger genes rarely contain pseudogenes, by contrast to other tandemly duplicated genes, perhaps because the modular structure of these proteins means that mutations in the Zn fingers can alter the specificity of their DNA binding sites without perturbing regulatory function or interactions with binding partners (Shannon et al., 2003). If HIM-8 and the ZIM proteins bind to their cognate chromosomes by a sequence-specific recognition mechanism, the sequences on the chromosomes are presumably also diverging to enable recognition by newly duplicated proteins. Characterization of the binding sites for these proteins will likely shed light on this dynamic process of chromosome specialization within the gene family.

In other species, chromosome attachment to the nuclear envelope during meiosis is mediated by telomeres. In *S. pombe* and *S. cerevisiae* this process requires telomere binding proteins shared by all chromosomes: Ndj1 in budding yeast and a complex including Rap1p, Taz1p, Bqt1p, and Bqt2p in fission yeast (Chikashige and Hiraoka, 2001; Chikashige et al., 2006; Cooper et al., 1998; Nimmo et al., 1998; Trelles-Sticken et al., 2000). Given that Ndj1 and Bqt1/2 do not appear to be broadly conserved, it is perhaps unsurprising that the PC binding proteins in *C. elegans* do not share obvious similarity with meiotic components from nonnematode species.

Hybridization of telomere probes to worm gonads has indicated the absence of a telomere-mediated meiotic bouquet (A.F.D., unpublished data). Together with the data presented here, this leads to the obvious hypothesis that the attachment of PCs to the nuclear envelope during meiosis has acquired the same function as the bouquet in other species. However, just what this function is remains enigmatic—the bouquet may help to bring homologs together, stabilize their interactions, and/or promote synapsis. Our observations that PCs do not cluster during meiosis suggests that the attachment of chromosome sites to the nuclear envelope may be more functionally relevant to the process of homolog pairing and synapsis than their clustering. Further analysis of the molecular basis of PC association with the nuclear envelope will likely clarify the fundamental mechanisms contributing to accurate homolog interactions during meiosis.

Experimental Procedures

Genetics and Mutant Alleles

Wild-type *C. elegans* (N2 Bristol) and all other strains were maintained under standard conditions at 20°C (Brenner, 1974). Deletion alleles of the three *zim* genes were generated and provided by the Japanese National Bioresource Project. One *zim-3* allele, *tm756*, is an in-frame deletion that disrupts the first of two zinc fingers. The other deletions, including *tm574*, *tm1813*, and *tm2303*, cause frame shifts that result in early stop codons. Based on sequence analysis, all of these alleles are predicted to result in complete loss of function of the corresponding gene, and this is supported by our phenotypic analysis, described above. All of the deletion mutations were found to be recessive; that is, no meiotic defects were detected in *zim*/+ heterozygotes. All mutations were outcrossed at least five times before analysis. Phenotypic analysis was carried out with homozygous mutant progeny from heterozygous parents to ensure that meiosis in the preceding generation was unperturbed and therefore that the animals we analyzed carried a euploid chromosome complement.

We were initially unable to generate adult animals homozygous for either of two deletion alleles of *zim-3* (*tm756* and *tm2303*). Homozygotes died as embryos or larvae, precluding analysis of their meiotic chromosome behavior. We initially suspected that ZIM-3 might play a more general role in development than the other ZIM/HIM-8 proteins. To test this idea, we generated animals that were heterozygous for *zim-3(tm756)* and deficiencies of the corresponding region of chromosome IV (*mDf7* and *sDf2*). These *zim-3(tm756)/Df* combinations produced viable, fertile adults, as did the trans-heterozygous combination of the two *zim-3* deletion alleles (*tm756/tm2303*). This indicates that the two *zim-3* alleles are associated with distinct lethal mutations and that the lethal mutation in the *zim-3(tm756)* strain is complemented by both of the chromosome IV deficiencies we tested. *tm756* appears to be associated with a closely linked chromosomal aberration that could not be separated from the deletion by recombination. However, we successfully separated *zim-3 (tm2303)* from a linked lethal by recombination in heterozygotes of the genotype *zim-3(tm2303)/unc-24 dpy-20 (IV)*. We recovered an Unc non-Dpy recombinant that carried *tm2303* and produced fertile, homozygous *unc-24 zim-3(tm2303)* progeny. The analysis reported here was performed with the resulting strain. Identical cytological defects were detected in *unc-24 zim-3(tm2303)* and trans-heterozygous *zim-3(tm756/tm2303)* animals, supporting the idea that both alleles result in loss of *zim-3* function, but the latter animals were not well suited to genetic assays due to the inviability of their *zim-3(tm756)* progeny.

In addition to the *zim* mutant alleles characterized here in detail, we examined the deletion T07G12.8 (*tm1479*). This mutation removes part of a large intron in the *zim-1* gene. This deletion did not result in complete loss of ZIM-1 expression, as judged by immunofluorescence, but did result in detectable defects in synapsis of chromosomes II and III, suggesting that it reduces expression of functional ZIM-1 protein.

Antibodies

Polyclonal antibodies were raised against peptides corresponding to unique, predicted antigenic regions of each ZIM protein. These peptides were: ZIM-1 (aa 568–596), SRQDKGSKRSQKSMDSGAKQKL DEARDED; ZIM-2 (aa 565–584), IGPVRKAERTPRRKLKSIRL; and ZIM-3 (aa 540–567), GKPRRYKKCKNSLKNTPEVDNENVDKDS. Rabbits and/or guinea pigs were immunized with each peptide. Crude antisera were used for all immunofluorescence experiments, except for ZIM-3, which was affinity purified against the ZIM-3 peptide. ZIM-1 serum was preadsorbed against formaldehyde-fixed wild-type worms to reduce nonspecific staining. Fluorescently conjugated secondary antibodies were purchased from Jackson ImmunoResearch or Molecular Probes.

Immunocytochemistry and FISH

DAPI-staining, FISH, and immunofluorescence were carried out as previously described (Phillips et al., 2005). FISH probes for *zim-2* pairing analysis were as follows. VR was synthesized from a pool of cosmids: T08C12, F26F2, W08A7, F46B3, and W01F3. VL was described by MacQueen et al. (2005) and was made from cosmids T27A9, T25C8, T12D8, and ZK526. The XC probe was a synthetic oligonucleotide of the sequence TTTCGCTTAGAGCGATTCCTTACCC TTAAATGGGCGCCGG, which is highly enriched on cosmid C07D8 (Lieb et al., 2000; Phillips et al., 2005). IIL (from Figure 2) and IIIL were made from cosmid pools F43C11, F53G2, and F59H5 (for IIL) and T19C3, K02F3, and W02B3 (for IIIL). IVC was made from a pool of four cosmids flanking but not including the *spo-11* gene. VR (from Figure 2) was made from a PCR-amplified 5S rDNA repeat as described by Dernburg et al. (1998). IIL (in Figure 6), IR, and IVL were generated from single fosmids: 33cD05, 37aC10, and 11cC03, respectively.

Most FISH probes were digested into small fragments with a mixture of restriction enzymes and then labeled by 3′ tailing with aminoallyl-dUTP. Amine-modified DNA was purified and conjugated to Cy3-NHS-ester, Cy5-NHS-ester (GE), or Alexa 488 or Oregon Green 488 succinimidyl-esters (Molecular Probes). Fosmid probes were 3′ end labeled with digoxigenin-dUTP (Roche) and detected with fluorescent anti-digoxin antibodies (Jackson ImmunoResearch) since this scheme provides somewhat higher sensitivity.

C. remanei and *C. briggsae* Sequencing and Gene Annotation

Using BLAST, we determined that the genomic region of *C. remanei* with homology to the *C. elegans* ZIM/HIM-8 operon is contained within supercontig6 of the 8/2005 preliminary release of the *C. remanei* genome. The published sequence contains three gaps, spanning Contig6.71, Contig6.72, Contig6.73, and Contig6.74. We designed primers to amplify across the gaps: GTGGTCTCGTTC AAAGTTCC and CATTTGACCGACAGTTTGGC for the first gap, AAACTTCAGTCATTCCGACTG and ATACCACGATCAACTTTCGTG for the second gap, and AGCAGCTCAGAAAACTACCC and GCTCTT CATTGAATGCATCC for the third gap. These regions were amplified by PCR with Bio-X-Act (Bioline) enzyme from *C. remanei* genomic DNA and sequenced. The sequences of these genomic PCR products have been entered into GenBank under accession numbers DQ493449–DQ493451 and are also provided as Supplemental Data. Also included is the genomic sequence of the entire gene cluster along with individual predicted cDNAs for the *C. remanei* genes. This information has been submitted to the GenBank TPA database under accession number BK005903.

A BAC clone (RPCI94_13P22) spanning the syntenic region of *C. briggsae* was obtained from the BAC/PAC Resource Center (http://bacpac.chori.org/). It was subcloned, shotgun sequenced, and assembled (GenBank accession #DQ498827).

To identify the *zim* and *him-8* genes in *C. briggsae* and *C. remanei*, we used the combined outputs of GenScan, GenomeScan, and GeneWise combined with manual editing to define ambiguous intron/exon boundaries, usually by bringing the paralogs into register (Birney et al., 2004; Burge and Karlin, 1997; Yeh et al., 2001). Where we observed discrepancies between the sequenced PCR products and the published nucleotide sequences from *C. remanei*, we used our experimentally determined sequences for gene annotations. Predicted cDNAs are included in GenBank TPA entry BK005903, as Supplemental Data (for *C. remanei*) and as GenBank accession number DQ498827 (for *C. briggsae*).

C. briggsae RNAi

Double-stranded RNA to inactivate the predicted *C. briggsae him-8* and *zim-4* genes was synthesized from PCR products generated with the following primers: TGCAATTTAGAAGTTCCGCG and GGA TAGGAATTGTAATCTCGC for *Cb-him-8* and CAAGTGAATATTTAC GGGCG and CATCTGACGATTTTTCAGACC for *Cb-zim-4*. The T7 promoter sequence (TAATACGACTCACTATAG) was added to the 5′ end of each primer so that double-stranded RNA could be directly synthesized from PCR products with the MEGAscript High Yield Transcription Kit (Ambion). PCR using *C. briggsae* genomic DNA template was carried out with Bio-X-Act enzyme (Bioline). Double-stranded RNA was transcribed in vitro from the PCR products with the MEGAscript High Yield Transcription Kit (Ambion). Annealed dsRNA was analyzed by agarose gel electrophoresis to verify size and integrity.

Adult *C. briggsae* hermaphrodites were injected with 1–5 mg/ml dsRNA as young adults, approximately 12 hr after the L4 larval stage. Injected animals were kept at 15°C for 20 hr and then transferred individually to new plates. Their F1 progeny were later transferred to individual plates and scored for meiotic phenotypes through cytological observations and brood analysis.

Supplemental Data

Supplemental Data include three figures and several DNA sequence files and are available online at http://www.developmentalcell.com/cgi/content/full/11/6/817/DC1/.

Acknowledgments

We are extremely grateful to Shohei Mitani and the Japanese National Bioresource for providing the deletion mutants described here. We also thank John Spieth, the BACPAC Resource Center, and especially Jan-Fang Cheng for providing BAC information and sequencing. Fosmids used for FISH probes were generated by the *C. elegans* Reverse Genetics Core Facility in Vancouver and graciously provided by Jaryn Perkins and Don Moerman. The SYP-1 and LMN-1 antibodies were generous gifts from Anne Villeneuve and Yossi Gruenbaum, respectively. We thank Gary Karpen, members of the Dernburg lab, and anonymous referees for

encouragement, helpful discussions, and constructive comments on the manuscript. This work was supported by a National Science Foundation predoctoral fellowship to C.M.P. and by National Institutes of Health R01 GM/CA655591 and Burroughs Wellcome Career Award 1000950 to A.F.D.

Received: June 6, 2006
Revised: September 8, 2006
Accepted: September 25, 2006
Published: December 4, 2006

References

Baker, B.S., Carpenter, A.T., Esposito, M.S., Esposito, R.E., and Sandler, L. (1976). The genetic control of meiosis. Annu. Rev. Genet. *10*, 53–134.

Bhalla, N., and Dernburg, A.F. (2005). A conserved checkpoint monitors meiotic chromosome synapsis in *Caenorhabditis elegans*. Science *310*, 1683–1686.

Birney, E., Clamp, M., and Durbin, R. (2004). GeneWise and Genomewise. Genome Res. *14*, 988–995.

Blumenthal, T., Evans, D., Link, C.D., Guffanti, A., Lawson, D., Thierry-Mieg, J., Thierry-Mieg, D., Chiu, W.L., Duke, K., Kiraly, M., and Kim, S.K. (2002). A global analysis of *Caenorhabditis elegans* operons. Nature *417*, 851–854.

Brenner, S. (1974). The genetics of *Caenorhabditis elegans*. Genetics *77*, 71–94.

Burge, C., and Karlin, S. (1997). Prediction of complete gene structures in human genomic DNA. J. Mol. Biol. *268*, 78–94.

Chenna, R., Sugawara, H., Koike, T., Lopez, R., Gibson, T.J., Higgins, D.G., and Thompson, J.D. (2003). Multiple sequence alignment with the Clustal series of programs. Nucleic Acids Res. *31*, 3497–3500.

Chikashige, Y., and Hiraoka, Y. (2001). Telomere binding of the Rap1 protein is required for meiosis in fission yeast. Curr. Biol. *11*, 1618–1623.

Chikashige, Y., Tsutsumi, C., Yamane, M., Okamasa, K., Haraguchi, T., and Hiraoka, Y. (2006). Meiotic proteins bqt1 and bqt2 tether telomeres to form the bouquet arrangement of chromosomes. Cell *125*, 59–69.

Colaiacovo, M.P., Stanfield, G.M., Reddy, K.C., Reinke, V., Kim, S.K., and Villeneuve, A.M. (2002). A targeted RNAi screen for genes involved in chromosome morphogenesis and nuclear organization in the *Caenorhabditis elegans* germline. Genetics *162*, 113–128.

Colaiacovo, M.P., MacQueen, A.J., Martinez-Perez, E., McDonald, K., Adamo, A., La Volpe, A., and Villeneuve, A.M. (2003). Synaptonemal complex assembly in *C. elegans* is dispensable for loading strand-exchange proteins but critical for proper completion of recombination. Dev. Cell *5*, 463–474.

Cooper, J.P., Watanabe, Y., and Nurse, P. (1998). Fission yeast Taz1 protein is required for meiotic telomere clustering and recombination. Nature *392*, 828–831.

Dernburg, A.F., McDonald, K., Moulder, G., Barstead, R., Dresser, M., and Villeneuve, A.M. (1998). Meiotic recombination in *C. elegans* initiates by a conserved mechanism and is dispensable for homologous chromosome synapsis. Cell *94*, 387–398.

Gengyo-Ando, K., and Mitani, S. (2000). Characterization of mutations induced by ethyl methanesulfonate, UV, and trimethylpsoralen in the nematode *Caenorhabditis elegans*. Biochem. Biophys. Res. Commun. *269*, 64–69.

Gerton, J.L., and Hawley, R.S. (2005). Homologous chromosome interactions in meiosis: diversity amidst conservation. Nat. Rev. Genet. *6*, 477–487.

Kiontke, K., Gavin, N.P., Raynes, Y., Roehrig, C., Piano, F., and Fitch, D.H. (2004). *Caenorhabditis* phylogeny predicts convergence of hermaphroditism and extensive intron loss. Proc. Natl. Acad. Sci. USA *101*, 9003–9008.

Lieb, J.D., de Solorzano, C.O., Rodriguez, E.G., Jones, A., Angelo, M., Lockett, S., and Meyer, B.J. (2000). The *Caenorhabditis elegans* dosage compensation machinery is recruited to X chromosome DNA attached to an autosome. Genetics *156*, 1603–1621.

MacQueen, A.J., and Villeneuve, A.M. (2001). Nuclear reorganization and homologous chromosome pairing during meiotic prophase require *C. elegans* chk-2. Genes Dev. *15*, 1674–1687.

MacQueen, A.J., Colaiacovo, M.P., McDonald, K., and Villeneuve, A.M. (2002). Synapsis-dependent and -independent mechanisms stabilize homolog pairing during meiotic prophase in *C. elegans*. Genes Dev. *16*, 2428–2442.

MacQueen, A.J., Phillips, C.M., Bhalla, N., Weiser, P., Villeneuve, A.M., and Dernburg, A.F. (2005). Chromosome sites play dual roles to establish homologous synapsis during meiosis in *C. elegans*. Cell *123*, 1037–1050.

McKim, K.S., Howell, A.M., and Rose, A.M. (1988). The effects of translocations on recombination frequency in *Caenorhabditis elegans*. Genetics *120*, 987–1001.

Nimmo, E.R., Pidoux, A.L., Perry, P.E., and Allshire, R.C. (1998). Defective meiosis in telomere-silencing mutants of *Schizosaccharomyces pombe*. Nature *392*, 825–828.

Phillips, C.M., Wong, C., Bhalla, N., Carlton, P.M., Weiser, P., Meneely, P.M., and Dernburg, A.F. (2005). HIM-8 binds to the X chromosome pairing center and mediates chromosome-specific meiotic synapsis. Cell *123*, 1051–1063.

Ross, L.O., Rankin, S., Shuster, M.F., and Dawson, D.S. (1996). Effects of homology, size and exchange of the meiotic segregation of model chromosomes in *Saccharomyces cerevisiae*. Genetics *142*, 79–89.

Scherthan, H. (2001). A bouquet makes ends meet. Nat. Rev. Mol. Cell Biol. *2*, 621–627.

Shannon, M., Hamilton, A.T., Gordon, L., Branscomb, E., and Stubbs, L. (2003). Differential expansion of zinc-finger transcription factor loci in homologous human and mouse gene clusters. Genome Res. *13*, 1097–1110.

Thompson, J.D., Higgins, D.G., and Gibson, T.J. (1994). CLUSTAL W: improving the sensitivity of progressive multiple sequence alignment through sequence weighting, position-specific gap penalties and weight matrix choice. Nucleic Acids Res. *22*, 4673–4680.

Trelles-Sticken, E., Dresser, M.E., and Scherthan, H. (2000). Meiotic telomere protein Ndj1p is required for meiosis-specific telomere distribution, bouquet formation and efficient homologue pairing. J. Cell Biol. *151*, 95–106.

Trelles-Sticken, E., Adelfalk, C., Loidl, J., and Scherthan, H. (2005). Meiotic telomere clustering requires actin for its formation and cohesin for its resolution. J. Cell Biol. *170*, 213–223.

Villeneuve, A.M. (1994). A cis-acting locus that promotes crossing over between X chromosomes in *Caenorhabditis elegans*. Genetics *136*, 887–902.

Yeh, R.F., Lim, L.P., and Burge, C.B. (2001). Computational inference of homologous gene structures in the human genome. Genome Res. *11*, 803–816.